Characterization of the Membrane Binding Mode of the C2 Domain of PKCϵ[†]

Senena Corbalán-Garcia,[‡] Susana Sánchez-Carrillo,[‡] Josefa García-García, and Juan C. Gómez-Fernández*

Department de Bioquímica y Biología Molecular (A), Facultad de Veterinaria, Universidad de Murcia, Apdo. 4021, E-30100 Murcia, Spain

Received May 21, 2003; Revised Manuscript Received July 25, 2003

ABSTRACT: PKCϵ is a member of the group of novel PKCs that contain a C2 domain located in their N-terminal region. On the basis of recent structural studies, a series of mutants were prepared to increase our knowledge of the mechanism of the phospholipid binding site of this domain. The results revealed that this domain preferentially binds to phosphatidic acid- and phosphatidylserine-containing vesicles. Although the increase in affinity was linear in the case of phosphatidic acid, it became exponential when the vesicles contained increasing concentrations of phosphatidylserine. Site-directed mutagenesis studies showed that residues W23, R26, and R32 located in loop 1 and I89 and Y91 located in loop 3 are of critical importance when the binding is performed with phosphatidic acid-containing vesicles. Furthermore, when the same mutants were assayed with phosphatidylserine-containing vesicles, no binding was observed in any case, reflecting the smaller affinity of the C2 domain for phosphatidylserine-containing vesicles. A study of the ionic nature of the membrane interaction suggested that it is mainly driven by electrostatic interactions that are disrupted by very low salt concentrations. Differential scanning calorimetry experiments performed to ascertain whether this interaction affected the transition phase of the phosphatidic acid demonstrated that increasing concentrations of the protein lead to changes in the transition, with more than one peak appearing at lower temperatures, which suggests a weak interaction focused on the polar headgroup of the phospholids. In conclusion, a different membrane-binding mode from those previously described in other C2 domains has been found and is seemingly based on electrostatic, interfacial, and hydrophobic interactions without the participation of Ca^{2+} ions.

PKC[1] molecules consist of a conserved catalytic C-terminal region common to all PKC isoforms and a more variable regulatory N-terminal region (*1*). In both classical and novel PKCs, the variable regulatory region is constituted by two types of molecular motifs—the C1 and C2 domains—which are targets for PKC activators. In addition, juxtaposed to the N-terminus of the C1 domains, the regulatory region contains a pseudosubstrate sequence that masks protein kinase activity in the absence of PKC activators (*2*). Membrane binding of novel PKCs does not require Ca^{2+}; in fact, they were not considered to be C2-domain-containing proteins until extensive sequence analysis suggested the possible presence of C2 sequence patterns preceding the C1 domains at the N-termini of the regulatory regions (*3*, *4*).

The structure of C2 domains, which are present not only in PKCs but also in a large variety of membrane-binding proteins, consists of a compact central β-sandwich composed of two four-stranded β-sheets (*5*−*12*). Connections at the top and at the bottom of the β-sandwich link the eight β-strands according to two distinct topologies (reviewed in *13* and *14*), although in general the C2 domains of novel PKCs, which do not require Ca^{2+}, exhibit a type II topology (*13*).

In vitro experiments have confirmed the ability of PKCϵ to bind to negatively charged phospholipid vesicles in a Ca^{2+}-independent manner, as has been seen for all other novel PKCs (*15*). However, the intrinsic mechanism driving this membrane interaction, together with the specificity for negatively charged phospholipids, is still not well defined.

The recently determined crystal structure of the C2 domain from PKCϵ has revealed important differences from novel PKCδ (*8*, *12*). Furthermore, the different behavior between PKCϵ and classical PKCs regarding membrane binding and activation appears to originate in localized structural changes, including the complete rearrangement of the region corresponding to the calcium binding pocket in classical PKCs (*12*).

Some previous studies carried out on PKCs from *Aplysia* of the classical and novel families have shown a certain implication of phosphatidic acid on the activation of these enzymes (*16*, *17*), although the precise amino acid residues from C2 involved in the activation have not been localized.

Here, we provide a detailed study of the phospholipid-binding mechanism of the C2 domain of PKCϵ. Using site-directed mutagenesis combined with fluorescence resonance

[†] This work was supported by Grant BMC2002-00119 from Dirección General de Investigación (Spain) and a grant from Fundación Séneca PI-35/00789/FS/01 (Comunidad Autónoma de Murcia) and Programa Ramón y Cajal from Ministerio de Ciencia y Tecnología and Universidad de Murcia (Spain) to S.C.-G..

* Corresponding author. E-mail: jcgomez@um.es. Tel: +34-968-364766. Fax: +34-968-364766.

[‡] These two authors contributed equally to this work.

[1] Abbreviations: FRET, fluorescence resonance energy transfer; PKC, protein kinase C; POPA, 1-palmitoyl-2-oleoyl-*sn*-glycero-3-phosphate; POPG, 1-palmitoyl-2-oleoyl-*sn*-glycero-3-phosphoglycerol; POPS, 1-palmitoyl-2-oleoyl-*sn*-glycero-3-phosphatidylserine.

10.1021/bi034850d CCC: $25.00
Published on Web 09/20/2003

energy transfer (FRET) and differential scanning calorimetry (DSC), we have analyzed the specific binding properties of this Ca^{2+}-independent C2 domain. The results demonstrate that PA and, to a lesser extent, PS can promote a membrane docking site for the domain and that the participation of loops 1 and 3 is crucial to the membrane interaction. In addition, differential scanning calorimetry experiments show that the protein-membrane binding induces slight changes in the transition temperature of the lipid, confirming the electrostatic nature of this interaction at the polar surface of the membrane.

MATERIALS AND METHODS

DNA Plasmids. The cDNA fragment corresponding to residues 1 to 138 of the rat PKCϵ-C2 domain, a kind gift from Drs. Nishizuka and Ono (Kobe University, Kobe, Japan), was amplified using PCR. The resulting 414 bp fragment was subcloned into the HindIII and BamHI sites of the bacterial expression vector pET28a(+), where the inserts were N-terminally fused to a tag of six histidines (6His). All constructs were confirmed by DNA sequencing. Variants of the PKCϵ-C2 domain were generated by PCR site-directed mutagenesis (*18*).

Expression and Purification of 6His-PKCϵ-C2. The pET28a(+) plasmid containing the PKCϵ-C2 domain was expressed and purified as previously described (*19*). Basically, the plasmids were transformed into BL21(DE3) *Escherichia coli* cells. The bacterial cultures (OD_{600} 0.6) were induced for 5 h at 30 °C with 0.5 mM of isopropyl-1-thio-β-D-galactopyranoside (IPTG) (Roche, Germany). The cells were lysed by sonication in lysis buffer (25 mM HEPES, pH 7.4, and 100 mM NaCl) containing protease inhibitors (10 mM benzamidine, 1 mM PMSF, and 10 μg/mL trypsin inhibitor). The soluble fraction of the lysate was incubated with Ni-NTA agarose (QIAGEN, Hilden, Germany) for 2 h at 4 °C. The Ni beads were washed with lysis buffer containing 20 mM imidazole. The bound fractions were eluted with the same buffer containing 250 mM imidazole. The 6His tag was removed after thrombin cleavage, and finally, the PKCϵ-C2 domain was desalted and concentrated using an Ultrafree-5 centrifugal filter unit (Millipore Inc., Bedford, MA). The protein concentration was determined using the BCA method (*20*).

Preparation of Lipid Vesicles. Lipid vesicles were generated by mixing chloroform solutions of 1-palmitoyl-2-oleoyl-*sn*-glycero-3-phosphocholine (POPC), *N*-(5-dimethylaminonaphthalene-1-sulfonyl)-1,2-dihexadecanoyl-*sn*-glycero-3-phosphoethanolamine (dansyl-DHPE), and 1-palmitoyl-2-oleoyl-*sn*-glycero-3-phosphate (POPA) or 1-palmitoyl-2-oleoyl-*sn*-glycero-3-phosphoserine (POPS) or 1-palmitoyl-2-oleoyl-*sn*-glycero-3-phosphoglycerol (POPG) (Avanti Polar Lipids, Inc., Alabaster, AL) in the desired proportions; the organic solvent was then removed under a nitrogen stream, and the vesicles were further dried under vacuum for 60 min. Dried phospholipids were resuspended in buffer containing 25 mM Hepes pH 7.4 and 0.5 mM EGTA by vigorous vortexing and were subjected to direct probe sonication (three cycles of 30 s).

Equilibrium Fluorescence Experiments. Equilibrium fluorescence experiments were carried out on an Fluoromax-3 fluorescence spectrometer at 25 °C in a standard assay buffer composed of 20 mM Hepes pH 7.4 and 10 mM KCl. The excitation and emission slit widths were 2 nm for all equilibrium fluorescence experiments. The phospholipid dependence of PKCϵ-C2 domain (0.5 μM) docking on the POPA, POPS, or POPG density was determined by increasing the mole percent of negatively charged phospholipid (PX) in a mixture with PC and dDHPE, keeping 5 mol % dDHPE constant while decreasing the concentration (mol %) of PC. Sonicated lipids were titrated in, and the protein-to-membrane FRET was monitored from the intrinsic tryptophan fluorescence emission at 340 nm using an excitation of 284 nm. Control experiments were performed under the same conditions in the absence of negatively charged phospholipids to discount the possibility of nonspecific binding. All total lipid concentrations were divided by 2 to take into account the inaccessibility of one of the leaflets to the protein because of the sealed nature of the bilamellar sonicated vesicles.

FRET was analyzed by using the equation proposed by Lakowicz, (*21*):

$$E = 1 - \frac{F}{F_0} \tag{1}$$

where F and F_0 are the donor fluorescence emission in the presence and in the absence of acceptor, respectively.

All equilibrium binding data were subjected to a nonlinear least-squares analysis using either the single independent site equation (eq 2) or the Hill equation (eq 3):

$$\Delta F = \Delta F_{max}\left(\frac{x}{K_D + x}\right) \tag{2}$$

$$\Delta F = \Delta F_{max}\left(\frac{x^H}{(\text{phospholipid})_{1/2}{}^H + x^H}\right) \tag{3}$$

ΔF_{max} represents the calculated maximal fluorescence change, x represents the free phospholipid concentration corrected for the leaflet effect (for phospholipid titrations), K_D represents the apparent equilibrium dissociation constant for lipid binding, $(\text{phospholipid})_{1/2}$ represents the negatively charged phospholipid concentration that yields half-maximal binding, and H is the Hill coefficient.

The effect of ionic strength on protein docking to the membrane was tested by titrating NaCl into samples containing the binary complex of the PKCϵ-C2 domain (0.5 μM) and vesicles (600 μM total PC, PA, and dDHPE; 65:30:5 mol %). The buffer that was used was standard buffer lacking KCl. The decreasing FRET signal was monitored. As a control, the isolated C2 domain of PKCα, which has been proposed to translocate to the vesicles electrostatically, was included in the assay (*22*). The contribution of the hydrophobic effect to docking was analyzed using the chaotropic salt Na_2SO_4, which enhances the hydrophobic effect (*23*, *24*). Na_2SO_4 was titrated into a mixture of the apo-C2 domain and vesicles (600 μM total PC, PA, and dDHPE; 65:30:5 mol %) in standard buffer, and membrane docking was monitored by protein-to-membrane FRET.

Gel-Filtration Binding Assay. Samples containing 80 μg of the PKCϵ-C2 domain and 320 μg of phospholipids labeled with [^{3}H]phosphatidylcholine were incubated in 100 μL of buffer containing 25 mM Hepes pH 7.4 and 10 mM KCl for 10 min. The sample was applied to a Sephadex G-100

(Sigma) column (1.0 cm × 2.5 cm) and was equilibrated and eluted (100 μL/fraction) with the same buffer. The phospholipid and protein elution profiles were detected as described by Garcia-Garcia et al. (*25*).

Differential Scanning Calorimetry. A high-sensitivity MicroCal MC-2 scanning calorimeter (Northampton, MA) was used in these experiments. Scan rates were 60°/h. The protein concentrations were 7.5, 30, and 75 μM for 200/1, 50/1, and 20/1 lipid/protein ratios, respectively. The lipid/protein mixtures were resuspended in 25 mM Hepes pH 7.4 and 0.5 mM EGTA, and a buffer profile was subtracted from the sample scans. Baselines were created by the cubic spline and subtracted. Calorimetric parameters T_c (temperature of the transition) and ΔH_{cal} (calorimetric enthalpy) were extracted from the data, and multiple peaks were fit with the Origin 5.0 software provided by MicroCal.

RESULTS AND DISCUSSION

Lipid Specificity of the PKCϵ-C2 Domain. The lipid specificity of the PKCϵ-C2 domain was determined by monitoring the protein-to-membrane FRET signal when lipids possessing different headgroups in different proportions were titrated into a solution of the C2 domain. Three different anionic lipid headgroups were tested, including PA, PS, and PG. All of the lipids were tested by titrating a mixture with PC at an increasing PC/PX mole ratio with a small amount (5 mol %) of the dansylated lipid dansyl-DHPE. As shown in Figure 1A, the C2-domain binding affinities increased with the percentage of POPA present in the phospholipid vesicles. The calculated apparent equilibrium dissociation constants (K_D) are shown in Table 1. These decreased from 313 μM at 10 mol % POPA to 20 μM when 60 mol % POPA was used in the assay, and a maximal FRET of 0.75 was obtained. Strikingly, when POPS was included in the assay, the PKCϵ-C2 domain exhibited low both binding affinity and FRET when the proportion of POPS ranged from 10 to 35 mol %. However, K_D decreased drastically to 54 and 29 μM when 40 and 60 mol % POPS were included in the vesicles, respectively. Furthermore, the experimental data exhibited a positive cooperativity and fit to the Hill equation better than a single independent site equation (Table 1). However, the maximal protein-to-membrane FRET was only 0.57, compared with 0.75 obtained when 60 mol % POPA was included in the vesicles, suggesting that although higher concentrations of POPS are able to increase the binding affinity of the domain POPA creates a better docking site at small concentrations of the phospholipid (20−30 mol %).

Because POPA and POPS exhibit only one net negative charge at physiological pH but both headgroups have quite different structures, with PS exhibiting a total of two negative charges plus one positive, these data suggest that the binding mechanism of the PKCϵ-C2 domain strongly depends on the establishment of specific interactions, besides the electrostatic switch mechanism. It is possible that PA creates a better docking site than PS at low concentrations. The capacity of PA to act at low concentrations would be in agreement with physiological events occurring, for example, upon activation of membrane receptors, when the percentage of generated PA represents only 5% of the total amount of PC existing in the plasma membrane and where PA has been identified as the activator (*26*). Low concentrations of PA (5 mol %) have also been observed to activate a novel PKC from *Aplysia* (*17*).

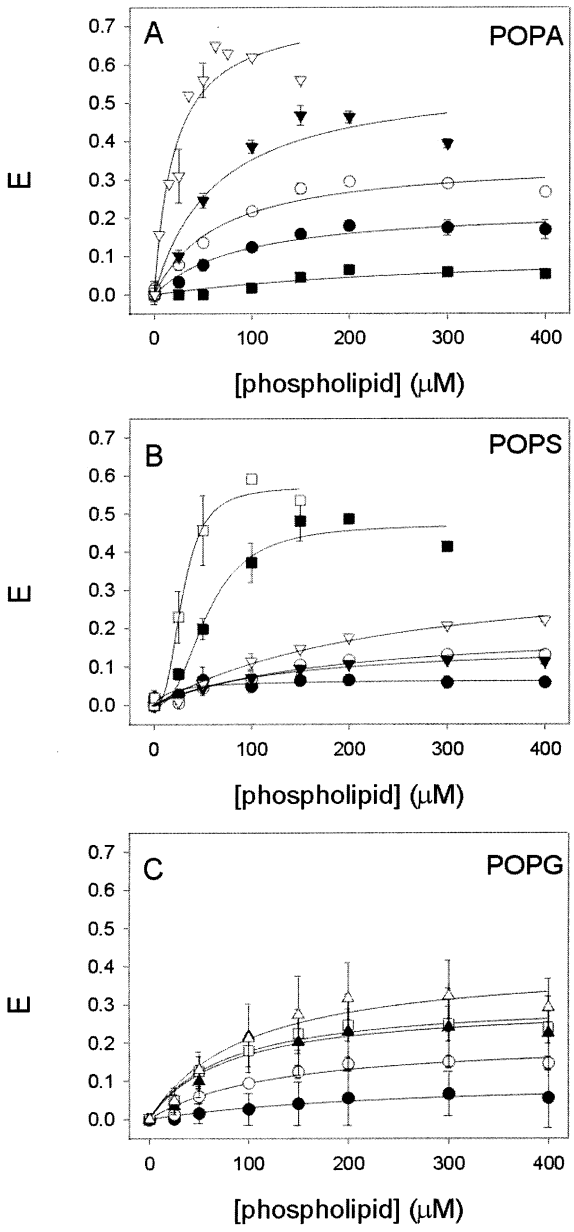

FIGURE 1: Phospholipid headgroup specificity of the PKCϵ-C2 domain. Phospholipid was titrated into solutions containing 0.5 μM PKCϵ-C2 domain. Vesicles were composed of a PC/PX/dhPE mixture, where PX is POPA (A), POPS (B), and POPG (C). The concentration of dhPE was kept constant at 5 mol %. In the case of POPA, 10 (■), 20 (●), 30 (○), 40 (▼), and 60 mol % (▽) were used. In the case of POPS, 10 (●), 20 (▼), 30 (○), 35 (▽), 40 (■), and 60 mol % (□) were used. In the case of POPG, 10 (●), 20 (○), 30 (▲), 40 (■), and 60 mol % (△) were used. Protein docking was assessed by protein-to-membrane FRET, using donor fluorescence to quantity the FRET. The solid lines represent the best fit of the resulting FRET signal to the equations described in the Materials and Methods section.

Whether the above results were only a matter of charges or whether a more specific docking site was involved was tested by including POPG in the lipid vesicles, which also exhibit one negative charge but contain a glycerol instead of the serine moiety. In this case, the binding affinity and the total protein translocation were very limited (Table 1). A protein-to-membrane FRET of 0.33 and a K_D of 64 μM were obtained when 60 mol % POPG was included in the

Table 1: Comparison of Equilibrium Affinity and Maximal Binding Parameters

	POPA		POPS			POPG	
% lipid	K_D	E_{max}	K_D	E_{max}	H_{Hill}	K_D	E_{max}
10	313	0.12	≫130	0.07		253	0.11
20	86	0.23	>130	0.20		123	0.21
30	65	0.35	130	0.16		76	0.31
35			125	0.37			
40	62	0.57	54	0.47	2.52	77	0.30
60	20	0.75	29	0.57	2.76	64	0.33

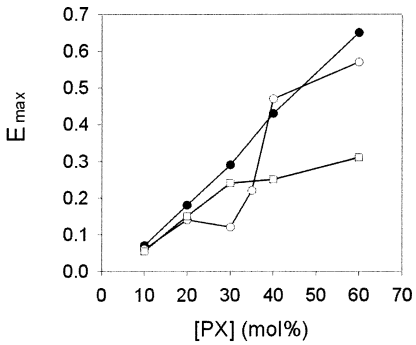

FIGURE 2: Dependency of maximal energy transfer on the percentage of anionic lipid composition of the vesicles. Maximal FRET is plotted versus the percentage of POPA (●), POPS (○), and POPG (□) included in the lipid vesicles. The linear dependence of FRET on POPA and the sigmoidal dependence of FRET on POPS can be clearly observed.

vesicles, suggesting that this phospholipid does not dock properly to the lipid-binding site of the C2 domain despite the fact that it confers negatively charged properties to the lipid vesicles.

Figure 2 shows a comparison of the E_{max} values obtained (Table 1) versus molar percentages of the three different negatively charged phospholipids. It should be remarked that whereas PA shows a linear dependence on its concentration PS has a sigmoidal dependence that may indicate the establishment of more than one interaction through its complex headgroup with a certain cooperativity. Taken together, these binding experiments clearly show that PA could be a very good promoter of membrane translocation of the PKCε-C2 domain even at low concentrations. The case of PS is striking because low concentrations of POPS produced a low degree of binding to the vesicles and only very high concentrations of the phospholipid were able to produce a degree of membrane binding with similar affinity to that of PA (Figure 2).

Roles of Loops 1 and 3 in the Membrane Docking of the PKCε-C2 Domain. According to the structure described in previous work (*12*), there are several potential residues, all of them concentrated in the β1-β2 (loop 1) and β5-β6 (loop 3) connections, that could be involved in phospholipid−protein interaction. To assess the role of these residues, we designed a mutagenesis strategy as follows: (a) the triple substitution of W23, R26, and R32 in loop 1 by A (PKCε-C2W23A/R26A/R32A); (b) the mutation of I89 located in loop 3 to N (PKCε-C2I89N); and (c) the mutation of Y91 (also located in loop 3) to A (PKCε-C2Y91A) (Figure 3A). Triple substitution in loop 1 was chosen because the single mutation of these residues had no effect on the binding properties of the domain (*12*).

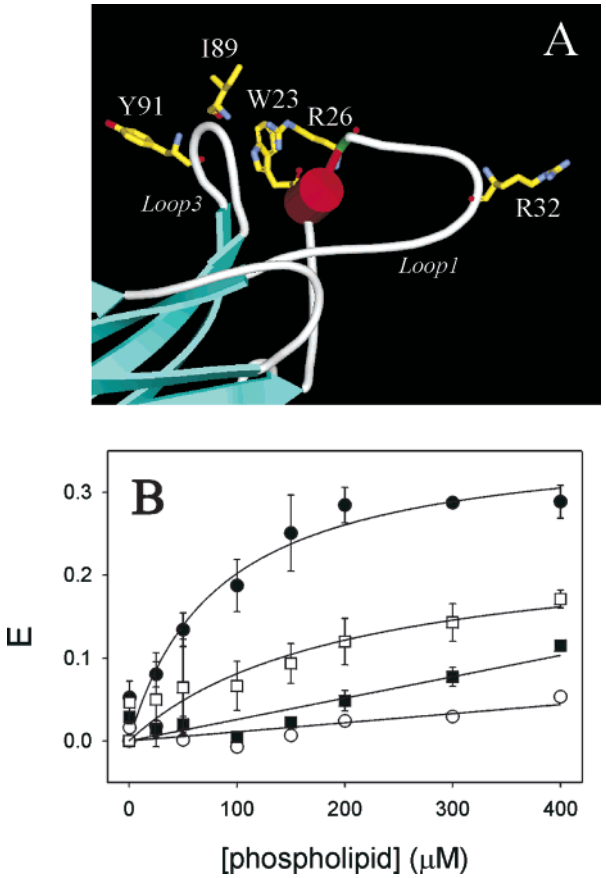

FIGURE 3: (A) Model structure of the lipid binding area of the PKCε-C2 domain. This model is based on the crystal structure solved by Ochoa et al. (*12*). Side chains of the residues possibly involved in lipid binding are depicted in yellow. The α-helix formed in loop 1 appears as a red cylinder. The program used was Swiss-PDB viewer 3.7 by GlaxoSmithKline (*32*). (B) Effect of the different amino acid substitutions on POPA binding. Vesicles were composed of a mixture of POPC/POPA/dhPE (65:30:5 mol %). Phospholipid was titrated into solutions containing 0.5 μM PKCε-C2 domain (●), PKCε-C2W23A/R26A/R32A (○), PKCε-C2I89N (■), and PKCε-C2Y91A (□).

We evaluated the contribution of these mutations to the interaction of PKCε-C2 with anionic phospholipid vesicles. Thus, we studied the dependence of phospholipid binding on the concentration of the phospholipid using 30 mol % POPA in the composition of the vesicles. This concentration was chosen because very high percentages of negatively charged phospholipids prevent differences between the wild-type protein and the mutants from being observed, apart from the fact that higher concentrations are out of the range of physiological conditions. Thus, maximal binding of the PKCε-C2 domain was obtained with 200 μM total lipid (Figure 3B). When the PKCε-C2W23A/R26A/R32A mutant was examined under the same conditions, no protein-to-membrane FRET was detected.

Among the three W residues existing in this domain, W23, which was substituted by A, is probably the only one involved in the lipid interaction. Therefore, the results observed after its mutation could be due to two reasons: (1) the mutation to A has abolished the source of the energy donor and (2) these residues are pivotal in membrane docking, their substitution completely abolishing protein−membrane binding. A molecular model based on the structure of the PKCε-C2 domain shows that the distances of the other

two W residues (W116 and W65) available in the molecule are also compatible with membrane FRET because they are located 26 and 18 Å, respectively, from the membrane surface (if we assume a parallel model) and at 29 and 22 Å, respectively, if we assume a perpendicular model of orientation of the protein (Figure 4A). Other evidence is shown in Figure 4B, where the fluorescence spectra of the PKCε-C2W23A/R26A/R32A mutant represent $^2/_3$ of the total fluorescence exhibited by the wild-type protein, suggesting that the W23A substitution affected only one of the residues.

To confirm that the PKCε-C2 domain binds to phospholipid vesicles containing 30 mol % POPA, the samples were also examined by gel-filtration chromatography using a Sephadex G-100 column. Figure 4C shows a binding assay, where the lipid elution profile was detected from the [^{3}H]-phosphatidylcholine contained in each fraction and the PKCε-C2 domain profile was determined by densitometry as described in the Materials and Methods section. As seen in Figure 4C, the elution profiles of the phosphatidic acid vesicles and PKCε-C2 domain overlapped, strongly suggesting that almost 100% of the domain was bound to lipids. In the case of the PKCε-C2W23A/R26A/R32A mutant, the lipid and protein profiles did not overlap, indicating that they were not bound (Figure 4D). Figure 4E shows a control of the elution profile of the PKCε-C2 domain in the absence of phospholipids, which correlates with nonbound protein. Taken together, all of these data suggest that the results obtained by FRET are due to the poor binding ability of the mutated protein rather than to the lack of fluorescence responsible for total FRET.

When the mutants located in loop 3 were tested, it was found that the substitution of I89 by N was very critical because only 32% of the maximal FRET was obtained. In the case of Y91 mutation to A, the effect was less drastic, and 55% of the maximal FRET was measured (Figure 3B), suggesting that under these conditions the I89 interaction with the phospholipid is more critical than the Y91 interaction.

Different results were obtained when POPS was included in the lipid vesicles. In this case, none of the mutants were able to translocate to the membrane. Taking into account that at 30 mol % POPS the affinity of the protein for the phospholipid is smaller than in the case of POPA, it is highly possible that the slight rearrangement introduced in the crevice by mutagenesis is responsible for such a damaging effect (Figure 5).

Taken together, these results demonstrate that residues located in both loops are critical to the membrane anchorage of the domain, probably through different types of interactions, one basically electrostatic and established by the R residues in loop 1 and other interfacial interactions performed by aromatic residues, such as W23 and Y91, located in loops 1 and 3, respectively. The existence of hydrophobic interactions through I89 cannot be ruled out because its substitution by N also has an important effect on membrane binding. The involvement of the aromatic residues, W23 and Y91, should be emphasized because it is widely recognized that these residues have a preference for membrane surfaces that is presumably due to the enhanced stability derived from their flat rigid shape and their aromaticity, factors that favor their location in close contact with the water−membrane interface (*27*). The involvement of this type of residue in

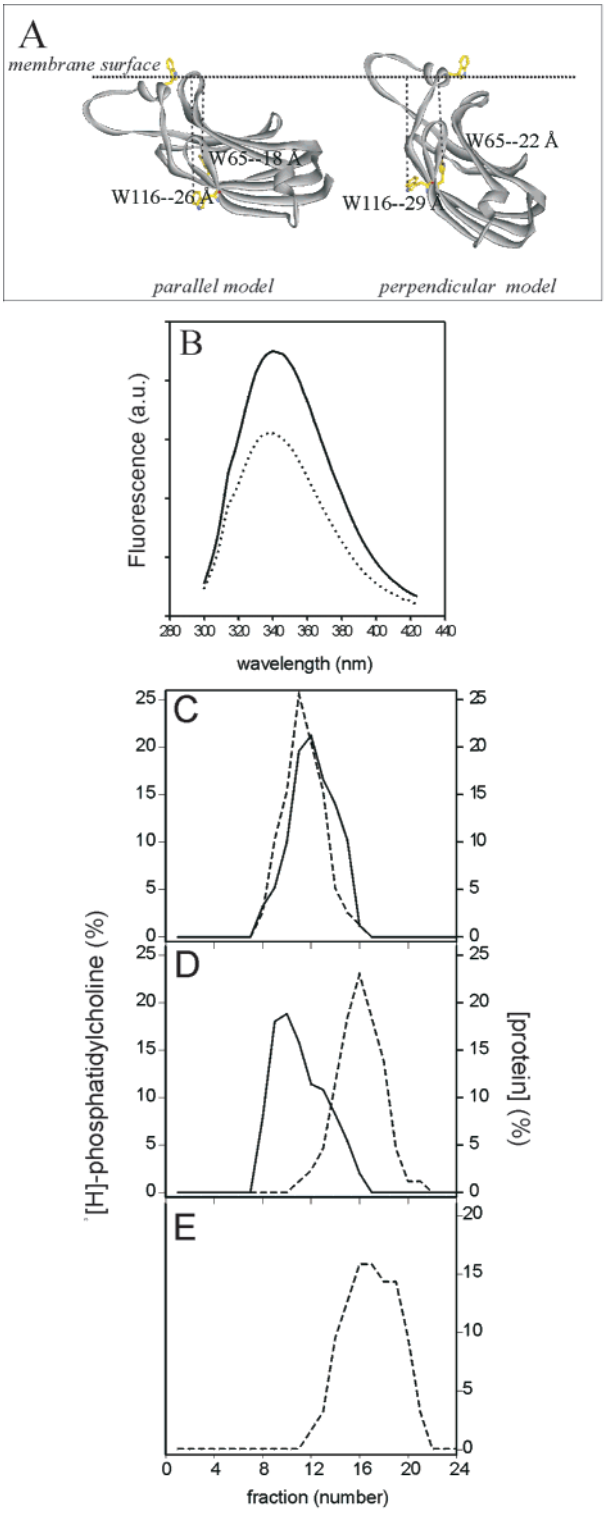

FIGURE 4: (A) Theoretical model to calculate the distances of the W residues located in the PKCε-C2 domain to the membrane surface. The program used was Swiss-PDB viewer 3.7 by Glaxo-SmithKline (*26*). (B) Fluorescence spectra of the PKCε-C2 domain (—) and PKCε-C2W23A/R26A/R32A (•••). (C) Determination of PKCε-C2 domain binding to 30 mol % POPA containing vesicles by gel filtration using a Sephadex G-100 column. The solid line represents the phospholipids' elution profile, and the dotted line represents the protein profile. (D) Determination of PKCε-C2 W23A/R26A/R32A domain binding to 30 mol % POPA containing vesicles by gel filtration using a Sephadex G-100 column. The solid line represents the phospholipids' elution profile, and the dotted line represents the protein profile. (E) Control experiment showing the elution profile of the PKCε-C2 domain in the absence of phospholipid vesicles (not bound protein).

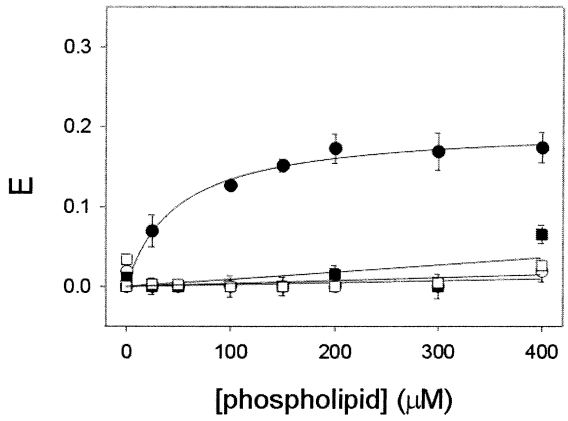

FIGURE 5: Effect of the different amino acid substitutions on POPS binding. Vesicles were composed of a mixture of POPC/POPS/dhPE (65:30:5 mol %). Phospholipid was titrated into solutions containing 0.5 μM PKCϵ-C2 domain (●), PKCϵ-C2W23A/R26A/R32A (○), PKCϵ-C2I89N (■), and PKCϵ-C2Y91A (□).

the interfacial docking of extrinsic membrane proteins has been observed, for example, in phospholipase A2 (*28*) and phosphatidylinositol-specific phospholipase C (*29*).

Electrostatic Nature of the Membrane Interaction. Previous studies have indicated that the binding of the C2 domains of classical PKCs to PS-containing membranes is largely electrostatic and the binding of the cytosolic phospholipase A2 C2 domain to membranes is primarily hydrophobic (*22*, *30*). To compare directly the forces driving the membrane docking of the PKCϵ-C2 domain, two experiments were conducted. First, NaCl was added to a preformed binary complex of the C2 domain and mixed PC/PA/dPE vesicles. Protein-to-membrane FRET measurements (Figure 6A) revealed that the addition of NaCl caused the dissociation of the PKCϵ-C2 domain at very low salt concentrations, suggesting that the affinity of the domain is highly electrostatic, even higher than that of the PKCα-C2 domain that needed at least 600 mM NaCl to dissociate from the membrane vesicles, as described previously by Kohout et al. (*22*). The second experiment tested the ability of sodium sulfate, which is known to strengthen hydrophobic interactions (*23*), to drive membrane docking. In this experiment, sodium sulfate failed to trigger protein-to-membrane FRET for the PKCϵ-C2 domain (Figure 6B), and increasing concentrations of the salt reduced to approximately 80% the membrane binding of the domain, confirming again the highly electrostatic nature of this protein−membrane interaction. In summary, these data suggest that the membrane docking of the PKCϵ-C2 domain is driven primarily by electrostatic interactions.

Effect of the PKCϵ-C2 Domain on the Phase Transition of Phosphatidic Acid. Previous studies in our laboratory have shown that the PKCϵ-C2 domain−phosphatidic acid interaction has a stabilizing effect on the protein, with the result that the denaturation transition cannot be detected because the protein structure is not modified by the increasing temperature (*19*).

Differential scanning calorimetry was used in this work to study the effect of the PKCϵ-C2 domain on the phase transition of POPA multilamellar vesicles (Figure 7). Pure POPA vesicles showed a gel-to-fluid phase-transition temperature (T_c) of 20.7 °C with a ΔH of 6.2 kcal/mol. When protein was added to provide a protein lipid molar ratio of

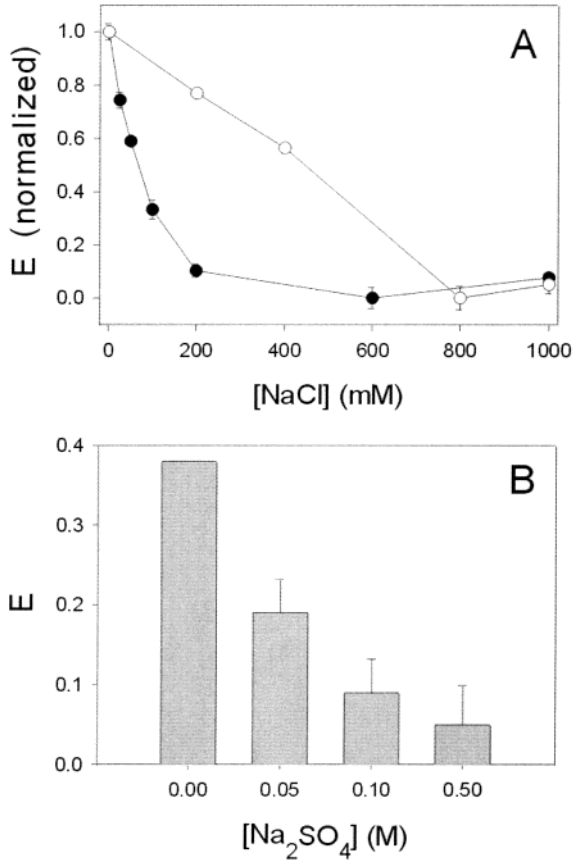

FIGURE 6: Ionic strength dependence of membrane docking. (A) NaCl was titrated into a solution of 0.5 μM PKCα-C2 domain (○) and PKCϵ-C2 domain (●) containing POPC/POPA/dhPE (65:30:5 mol %) in all cases and EGTA or 200 μM $CaCl_2$ for PKCϵ-C2 and PKCα-C2 domains, respectively. The FRET signal was normalized to the initial FRET signal in the absence of added NaCl. (B) The PKCϵ-C2 domain and POPC/POPA/dhPE (65:30:5 mol %) vesicles were incubated with 0.05, 0.1, and 0.5 M Na_2SO_4.

1:200, the phase transition produced a peak with a shoulder. This peak was decomposed into two components, of which the larger had a T_c of 20.7 °C and a ΔH of 4.61 kcal/mol and the smaller had a T_c of 21.8 °C and a ΔH of 1.46 kcal/mol. Given the observed T_c transition temperatures, it may be deduced that the component with a T_c of 20.7 °C corresponds to pure POPA, whereas 21.8 °C corresponds to POPA molecules interacting with the protein. Note that by adding the ΔH values of the two components the total value obtained is practically equal to the ΔH of the pure POPA for the samples with 1:200 and 1:50 P/L molar ratios. The sample with a protein/POPA molar ratio of 1:50 also showed a peak with a small shoulder representing two components with T_c values of 21.8 and 20.7 °C and ΔH values of 1.24 and 4.6 kcal/mol, respectively. Again, it seems that the larger component corresponds to pure POPA. A further increase in protein concentration to provide a protein lipid molar ratio of 1:20 resulted in a transition peak of two clearly separated components, the first with a T_c of 20.8 °C (ΔH of 1.5 kcal/mol) and the second with a T_c of 19.3 °C (ΔH of 4.4 kcal/mol). The appearance of a second transition peak in the three samples containing protein, unlike that seen in pure phospholipid, and at the same time the small effect on the size of the transition peak point to an interaction in the polar headgroup region rather than in the hydrophobic membrane palisade. This is a type D profile, as classified by Jain and

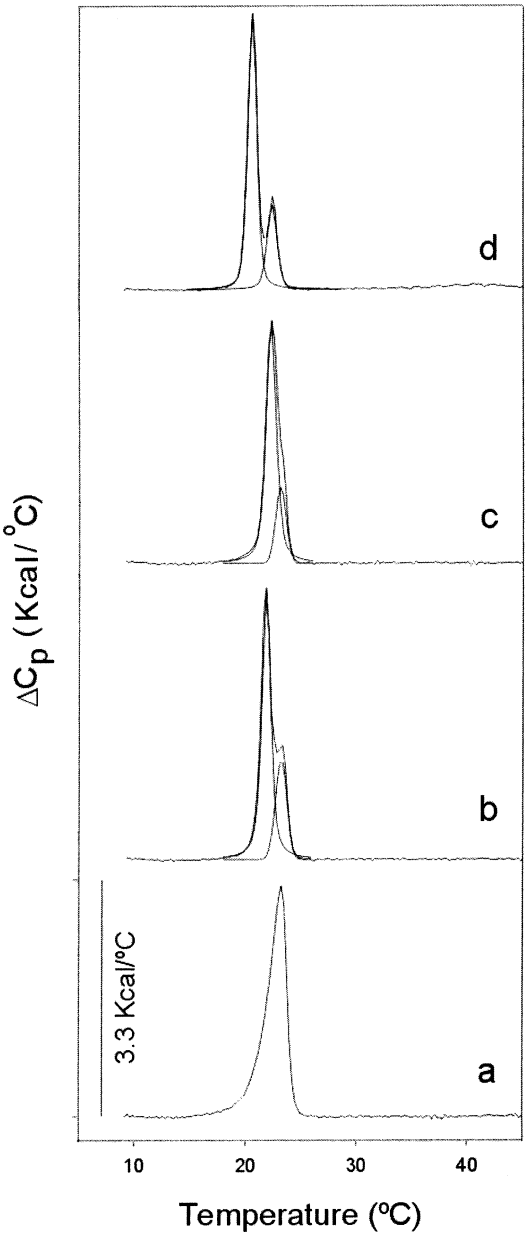

FIGURE 7: DSC thermograms for POPA vesicles (100 mol %) in the absence (a) of the PKCϵ-C2 domain and in the presence of protein at 1/200 (b), 1/50 (c), and 1/20 (d) P/L molar ratios. The increase in heat capacity (ΔC_p) was 3.3 K cal/°C. The total lipid concentration was 1.5 mM.

Wu (*31*), a type of profile that usually results from a change in the packing within the cooperative unit while the size of the cooperative unit remains essentially unchanged. Nevertheless, and given the very small modification in the T_c value of the modified phospholipid with respect to the value of the unperturbed species, the conclusion is that the packing does not change very much.

CONCLUSIONS

Taken together, the mutational data suggest that loops 1 and 3 are essential to the interaction between the C2 domain and phospholipids, preferentially phosphatidic acid. Thus, the PKCϵ-C2 domain exhibits a new binding mechanism because translocation to the plasma membrane is Ca^{2+}-independent but exhibits three components, the first being an electrostatic force that will be established through specific interactions because not all negatively charged phospholipids produce protein−membrane interactions to the same extent and with the same affinity. The second component is the additional interfacial interactions performed by aromatic residues located both in loops 1 and 3, and the third component is a limited hydrophobic interaction that is probably established by the residues located in loop 3, which seems to be less essential than the electrostatic component. However, from the results obtained both through competition with NaCl and through DSC, it seems that the PKCϵ-C2 domain does not penetrate the membrane bilayer very deeply, so the interaction probably takes place with the segment of the acyl chains close to the carbonyl groups of the phospholipid.

ACKNOWLEDGMENT

We thank Drs. Ono and Nishizuka (Kobe, Japan) for the kind gift of the cDNA coding for PKCϵ.

REFERENCES

1. Newton, A. C., and Johnson, J. E. (1998) *Biochim. Biophys. Acta 1376*, 155−172.
2. Newton, A. C. (2001) *Chem. Rev. 101*, 2353−2364.
3. Sossin, W. S., and Schwartz, J. H. (1993) *Trends Biochem. Sci. 18*, 207−208.
4. Ponting, C. P., and Parker, P. J. (1996) *Protein Sci. 5*, 162−166.
5. Sutton, R. B., Davletov, B. A., Berghuis, A. M., Südhof, T. C., and Sprang, S. R. (1995) *Cell 80*, 929−938.
6. Essen, L.-O., Perisic, O., Cheung, R., Katan, M., and Williams, R. L. (1996) *Nature 380*, 595−602.
7. Sutton, R. B., and Sprang, S. R. (1998) *Structure 6*, 1395−1405.
8. Pappa, H., Murray-Rust, J., Dekker, L. V., Parker, P. J., and McDonald, N. Q. (1998) *Structure 6*, 885−894.
9. Perisic, O., Fong, S., Lynch, D. E., Bycroft, M., and Williams, R. L. (1998) *J. Biol. Chem. 273*, 1596−1604.
10. Verdaguer, N., Corbalan-Garcia, S., Ochoa, W. F., Fita, I., and Gómez-Fernández, J. C. (1999) *EMBO J. 18*, 6329−6338.
11. Dessen, A., Tang, J., Schmidt, H., Stahl, M., Clark, J. D., Seehra, J., and Somers, W. S. (1999) *Cell 97*, 349−360.
12. Ochoa, W. F., Garcia-Garcia, J., Fita, I., Corbalan-Garcia, S., Verdaguer, N., and Gomez-Fernandez, J. C. (2001). *J. Mol. Biol. 311*, 837−849.
13. Nalefski, E. A., and Falke, J. J. (1996). *Protein Sci. 5*, 2375−2390.
14. Rizo, J., and Südhof, T. C. (1998) *J. Biol. Chem. 273*, 15879−15882.
15. Medkova, M., and Cho, W. (1998) *Biochemistry 37*, 4892−4900.
16. Pepio, A. M., and Sossin, W. S. (1998) *Biochemistry 37*, 1256−1263.
17. -Pepio, A. M., Fan, X., and Sossin, W. S. (1998) *J. Biol. Chem. 30*, 19040−19048.
18. Saiki, R. K., Gellan, D. H., Stoftel, S., Scharf, S. J., Higuchi, R., Horn, G. T., Mullis, K. B., and Erlich, H. A. (1988) *Science 235*, 487−491.
19. Garcia-Garcia, J., Gomez-Fernandez, J. C., and Corbalan-Garcia, S. (2001) *Eur. J. Biochem. 268*, 1107−1117.
20. Smith, P. K., Krohn, R. I., Hermanson, G. T., Mallia, A. K., Gartner, F. H., Provenzano, M. D., Fujimoto, E. K., Goeke, N. M., Olson, B. J., and Klenk, D. C. (1985). *Anal. Biochem 150*, 76−85.
21. Lakovicz, J. R. (1983) *Principles of Fluorescence Spectroscopy*, Plenum Publishing Corp., New York.
22. Kohout, S. C., Corbalán-García, S., Torrecillas, A., Gómez-Fernández, J. C., and Falke, J. J. (2002) *Biochemistry 41*, 11411−24.
23. Nalefski, E. A., McDonagh, T., Somers, W., Seehra, J., Falke, J. J., and Clark, J. D. (1998) *J. Biol. Chem. 273*, 1365−1372.
24. Creighton, T. E. (1993) *Proteins: Structures and Molecular Properties*, 2nd ed., W. H. Freeman, New York.
25. Garcia-Garcia, J., Corbalan-Garcia, S., and Gomez-Fernandez, J. C. (1999) *Biochemistry 38*, 9667−9675.

26. Buckland, A. G., and Wilton, D. C. (2000) *Biochim. Biophys. Acta 1483*, 199−216.
27. Yan, W. M., Wimley, W. C., Gawrisch, K., and White, S. H. (1998) *Biochemistry 37*, 14713−14718.
28. Sumandea, M., Das, S., Sumandea, C., and Cho, W. (1999) *Biochemistry 38*, 16290−16297.
29. Feng, J., Webhi, H., and Roberts, M. F. (2003) *J. Biol. Chem 277*, 19867−19875.
30. Murray, D., and Honig, B. (2002) *Mol. Cell. 9*, 145−54.
31. Jain, M. K., and Wu, N.-N. (1977) *J. Membr. Biol. 34*, 157−201.
32. Guex, N., and Peitsch, M. C. (1997) *Electrophoresis 18*, 2714−2723.

BI034850D